

GRAVITY OFFSET AND COUPLING FACTOR OF MIXED MODES IN RGB STARS

C. Pinçon¹

Abstract. The space-borne missions CoRoT and *Kepler* provided us with exquisite photometric data for thousands of red giant stars. The observation of mixed modes in the oscillation spectra of these stars brought stringent constraints on their deep interiors. In this short article, we discuss the potential of two seismic parameters associated with mixed modes, namely, the gravity offset, ε_g , and coupling factor, q , to probe the internal structure of red giants. The observed variations in these parameters along the red giant branch (hereafter, RGB) are interpreted by means of a simple analytical model. Their sensitivity to the extra mixing at the base of the convective envelope (hereafter, BCZ) is emphasized.

Keywords: asteroseismology, stellar interior, stellar modeling

1 Mixed-mode frequency pattern

Owing to the high density contrast between the core and the envelope of red giant stars, stochastically-excited oscillation modes can propagate in two resonant cavities: a central one where they behave as gravity waves, and an external one where they behave as acoustic waves. Both resonant cavities are coupled by an intermediate region where the modes are evanescent (hereafter, ER for evanescent region), that is, where the mode frequency is larger than the Brunt-Väisälä frequency but smaller than the Lamb frequency. Such modes constitute the so-called mixed modes (e.g., Hekker & Christensen-Dalsgaard 2017, for a recent review). Guided by the asymptotic theory (i.e., in the short-wavelength approximation) of stellar oscillations (e.g., Shibahashi 1979; Tassoul 1980; Takata 2016a), observations showed that the frequency pattern of mixed modes is ruled at leading order by the implicit quantization condition (e.g., Mosser et al. 2012, 2018)

$$\cot \left[\pi \left(\frac{1}{\nu \Delta \Pi} - \varepsilon_g \right) \right] \tan \left[\pi \left(\frac{\nu}{\Delta \nu} - \varepsilon_p(\nu) \right) \right] = q, \quad (1.1)$$

where ν is the mode frequency, and $\Delta \Pi$, $\Delta \nu$, q , and ε_g are frequency-independent parameters representing the period spacing, large frequency separation, coupling factor and gravity offset, respectively. Besides, the acoustic offset $\varepsilon_p(\nu)$ is supposed to follow the quadratic universal red-giant oscillation pattern for pressure modes (e.g., Mosser et al. 2011).

According to the asymptotic theory of mixed modes, $\Delta \Pi$ and $\Delta \nu$ are related to the “size” (i.e., as seen by waves) of the internal and external cavities, respectively. Moreover, q measures the transmission of the wave energy from one cavity to the other one through the intermediate ER, while ε_g and ε_p are sensitive to the phase lags induced at the wave reflection near the boundaries of the inner cavity (i.e., at the center and the inner edge of the ER) and those of the external cavity (i.e., at the outer edge of the ER and at the surface), respectively (e.g., Takata 2016b). The mixed-mode frequency pattern has thus the potential to bring us information on the properties of the whole structure of RGB stars, that is, of their core, envelope, and mid-layers. As an illustration, a synthetic frequency spectrum obtained by solving Eq. (1.1) with typical parameters is represented in a period-échelle diagram and plotted in Fig. 1 (left panel).

Before going further, it is worth mentioning that Eq. (1.1) is an approximate form of the asymptotic expression of mixed modes over a narrow frequency range around ν_{\max} , the frequency at maximum oscillation power (e.g, Belkacem et al. 2011). Interpreting the fitted values of the parameters within the asymptotic framework is thus relevant if the observational error bars are larger than the error made when approximating the asymptotic expression by Eq. (1.1). We assume in the following that this condition is always met, given that the typical observed frequency ranges in red giant stars are quite narrow around ν_{\max} (e.g., see Fig. 5 of Mosser et al. 2013).

¹ STAR Institute, Université de Liège, 19C Allée du 6 Août, B-4000 Liège, Belgium

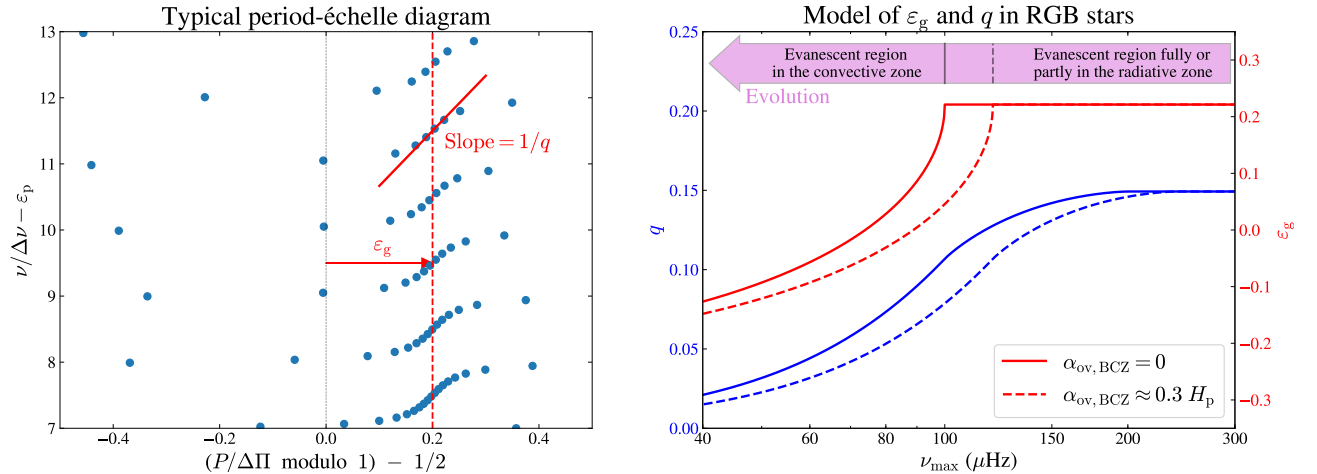


Fig. 1. Left: Period-échelle diagram obtained by solving Eq. (1.1) for a typical Red Giant where $\Delta\nu = 10 \mu\text{Hz}$, $\nu_{\text{max}} = 100 \mu\text{Hz}$, $\Delta\Pi = 100 \text{ s}$, $\varepsilon_g = 0.2$, $q = 0.12$ and ε_p is frequency-dependent. Each blue dot represents an oscillation mode. The influence of ε_g and q on the shape of the spectrum is emphasized. **Right:** Model for the coupling factor and gravity offset on the RGB (blue and red, respectively) for typical values of ν_{max} . Evolution goes from the right to the left. Dashed lines represent the predictions when an adiabatic overshooting region is included at the BCZ.

2 Physical interpretation of the observed values of ε_g and q

2.1 Asymptotic predictions in a simple model

The asymptotic expressions of q and ε_g essentially depend on the properties of the ER. As shown by typical stellar models, the intermediate ER is located in the upper part of the radiative zone at the beginning of the RGB, that is, between the hydrogen-burning shell and the BCZ. As ν_{max} decreases during the evolution on the RGB, the ER progressively migrates toward the lower part of the convective region (e.g., Hekker et al. 2018; Pinçon et al. 2019b). In order to explicitly express the asymptotic forms of these parameters as a function of the stellar properties, reasonable assumptions about the structure of the ER can be made along the evolution on the RGB. We note that this study implicitly focuses on dipolar modes since they are the most easily observable and were detected for a large sample of stars.

First, owing to the high density contrast between the core and surface of RGB stars, the internal structure (i.e., pressure, density,...) can be supposed in a good approximation to follow power laws with respect to radius in the ER. In these considerations, the Brunt-Väisälä frequency is about twice lower than the Lamb frequency, but their power-law exponents are similar and close to $-3/2$, except for the Brunt-Väisälä frequency in the convective zone that vanishes. Second, the ER can be supposed to be thick and the low-coupling formalism of Shibahashi (1979) has to be considered. Moreover, guided by stellar models, we assume that the envelope expansion is so predominant that the changes in the properties of the ER are much more related to its progressive migration during the RGB (owing to the rapid decrease in ν_{max}) rather than the slower evolution of the mid-layer structure. Finally, the ER is assumed to become fully located in the lower part of the convective envelope when $\nu_{\text{max}} \lesssim 100 \mu\text{Hz}$. We refer the reader to Pinçon et al. (2019a) for more details. Using this modeling, Pinçon et al. (2019a,b) could predict the evolution of the asymptotic expressions of q and ε_g on the RGB.

As shown in Fig. 1 (right panel), the model predicts that the gravity offset remains about equal to 0.22 in the first part of the RGB when the ER is located in the radiative region (i.e., for $100 \mu\text{Hz} \leq \nu_{\text{max}} \lesssim 300 \mu\text{Hz}$). This is a direct consequence of the power-law behavior of the structure. As soon as the ER arrives in the convective zone, the asymptotic value of ε_g sharply drops; it then continues to progressively decrease during the rest of the evolution on the RGB. This sudden change originates from the abrupt kink of the profile of the Brunt-Väisälä frequency at the BCZ. These predictions are in global agreement with the observations of Mosser et al. (2018): the drop in the observed value of the gravity offset around $\nu_{\text{max}} \sim 100 \mu\text{Hz}$ can therefore be interpreted as the signature of the arrival of the whole ER in the lower part of the convective envelope.

In contrast, Fig. 1 (right panel) shows that q is expected to smoothly decrease during the evolution on the RGB. More precisely, for $200 \mu\text{Hz} \lesssim \nu_{\text{max}} \lesssim 300 \mu\text{Hz}$, q remains equal to about 0.14 as a result, again, of the power-law behavior of the structure in the ER. Later on the RGB, that is, for $100 \mu\text{Hz} \lesssim \nu_{\text{max}} \lesssim 200 \mu\text{Hz}$, q starts decreasing slowly, because of the progressive migration of the ER in the vicinity of the BCZ. When

the ER becomes fully located in the convective zone, that is, for $\nu_{\max} \lesssim 100 \mu\text{Hz}$, the predicted decrease in q results from the continuous increase in the radial thickness of the ER as ν_{\max} decreases, so that the coupling between the two resonant cavities lowers. These predictions turn out to be in qualitative agreement with the observations of Mosser et al. (2017). The decreasing trend in the observed values of the coupling factor can therefore be interpreted as the result of either the progressive migration of the ER from the radiative to the convective regions for $\nu_{\max} \gtrsim 100 \mu\text{Hz}$, or the increase in the thickness of the ER for $\nu_{\max} \lesssim 100 \mu\text{Hz}$. We nevertheless note that the model predicts too small values of q compared to observations in evolved red giant stars (i.e., for $\nu_{\max} \lesssim 100 \mu\text{Hz}$). This quantitative discrepancy could result from an observational bias, buoyancy glitches, or the frequency dependence of q over the observed frequency range (e.g., Cunha et al. 2019; Pinçon et al. 2019a).

2.2 Influence of overshooting at the BCZ

At a given evolutionary state (i.e., at a given value of ν_{\max}), accounting for overshooting moves the BCZ toward deeper layers. As a result, the ER reaches the convective zone earlier on the RGB. Using typical stellar models, Pinçon et al. (2019b,a) found that including an adiabatic overshooting region over about $0.3H_p$ at the BCZ, with H_p the local pressure scale height, increases the value of ν_{\max} at which the whole ER arrives in the convective zone from about $100 \mu\text{Hz}$ to about $120 \mu\text{Hz}$. We note that Khan et al. (2018) demonstrated that such a value of overshooting is needed to fit the luminosity bump on the RGB. We can see in Fig. 1 (right panel) that overshooting tends to decrease the values of ε_g and q at a given value of ν_{\max} . Moreover, the characteristic sharp decrease in ε_g occurs at higher values of ν_{\max} . These predictions clearly demonstrate the potential of these parameters to probe the convective mixing processes at the BCZ.

3 Concluding remarks

The link between the global variations observed in q and ε_g and the migration of the ER from the radiative to the convective regions on the RGB is now demonstrated. The sensitivity of these parameters to the extra mixing at the BCZ is clearly emphasized. As a next step, a more detailed study of q and ε_g in grids of stellar models or in observed RGB stars with high signal-to-noise ratio will have to be performed to assess quantitatively and practically the potential of these parameters as seismic diagnoses of the stellar interior.

C. P. warmly thanks M. Takata, B. Mosser, M.-J. Goupil and K. Belkacem for fruitful discussions about the present topic, as well as M. Farnir for his careful reading of the paper. During this work, C. P. was funded by a postdoctoral fellowship from F.R.S.-FNRS.

References

- Belkacem, K., Goupil, M. J., Dupret, M. A., et al. 2011, *A&A*, 530, A142
 Cunha, M. S., Avelino, P. P., Christensen-Dalsgaard, J., et al. 2019, *MNRAS*, 2220
 Hekker, S. & Christensen-Dalsgaard, J. 2017, *A&A Rev.*, 25, 1
 Hekker, S., Elsworth, Y., & Angelou, G. C. 2018, *A&A*, 610, A80
 Khan, S., Hall, O. J., Miglio, A., et al. 2018, *ApJ*, 859, 156
 Mosser, B., Belkacem, K., Goupil, M. J., et al. 2011, *A&A*, 525, L9
 Mosser, B., Gehan, C., Belkacem, K., et al. 2018, *A&A*, 618, A109
 Mosser, B., Goupil, M. J., Belkacem, K., et al. 2012, *A&A*, 540, A143
 Mosser, B., Pinçon, C., Belkacem, K., Takata, M., & Vradar, M. 2017, *A&A*, 600, A1
 Mosser, B., Samadi, R., & Belkacem, K. 2013, in *SF2A-2013: Proceedings of the Annual meeting of the French Society of Astronomy and Astrophysics*, ed. L. Cambresy, F. Martins, E. Nuss, & A. Palacios, 25–36
 Pinçon, C., Goupil, M. J., & Belkacem, B. 2019a, submitted to *A&A*
 Pinçon, C., Takata, M., & Mosser, B. 2019b, *A&A*, 626, A125
 Shibahashi, H. 1979, *PASJ*, 31, 87
 Takata, M. 2016a, *PASJ*, 68, 109
 Takata, M. 2016b, *PASJ*, 68, 91
 Tassoul, M. 1980, *ApJ*, 43, 469